Journal of Physics: Conference Series **381** (2012) 012020 doi:10.1088/1742-6596/381/1/012020

Nuclear Force and Nuclear Physics from Lattice Quantum Chromodynamics

Tetsuo Hatsuda

Phys. Dep., Univ. of Tokyo, Tokyo 113-0033, Japan
IPMU, Univ. of Tokyo, Chiba 277-8583, Japan
Theoretical Research Division, Nishina Center, RIKEN, Saitama 351-0198, Japan

E-mail: thatsuda@riken.jp

Abstract. Recent progress in lattice QCD is reviewed with special emphasis on the lattice nuclear force and lattice baryon forces.

1. Introdution

Quantum chromodynamics (QCD) is the theory of strong interaction described by the Langragian density:

$$\mathcal{L} = -\frac{1}{4} G^a_{\mu\nu} G^{\mu\nu}_a + \sum_{f=1}^{n_f} \bar{q}_f \gamma^\mu (i\partial_\mu - g t^a A^a_\mu - m_f) q_f. \tag{1}$$

It is well established at high energies using perturbative QCD and factorization theorems and at low energies using lattice QCD. Therefore, the current issue is not to check the validity of QCD but to solve QCD to have a better understanding of the many-body physics in particle physics, nuclear physics and astrophysics such as

- quark structure of hadrons and nuclei,
- origin of the heavy elements in explosive astrophysical phenomena,
- physics of the primordial form of matter, the quark-gluon plasma,
- structure of the super dense matter such as the neutron stars,
- constraints on the theories beyond the standard model.

Lattice QCD, which has shown tremendous progress over the past 10 years, can provide us with not only precision computations but also qualitative pictures to understand the above issues.

2. Precision Lattice QCD

QCD can be formulated in a well-defined way on the hypercubic lattice with the lattice spacing a and the lattice volume L. The gluons and quarks are defined on the links and the sites, respectively. To make comparison to experimental observables, extrapolation of the numerical results to the continuum limit $a \to 0$ and the thermodynamic limit $L \to \infty$ must be taken.

Progress in numerical algorithms together with the increase of supercomputer performance enable us to make in (2+1)-flavour full QCD simulations already possible at the physical point $m_\pi = 135$ MeV [1, 2].

In Eq.(1), there are only two kinds of parameters, the QCD coupling constant g and the quark masses m_f. They are the fundamental parameters and can be determined by calculating several in lattice QCD simulations. The latest compilation of the running coupling at the Z-pole in the $\bar{M}S$-scheme from lattice QCD reads [3]

$$\alpha_s^{(5)}(M_Z) = 0.1189^{+4}_{-6}. \tag{2}$$

The quark masses at the 2 GeV scale in the $\bar{M}S$-scheme from (2+1)-flavour lattice QCD with estimated QED corrections read [4]

$$m_u = 2.19(15)\ \text{MeV},\ \ m_d = 4.67(20)\ \text{MeV}, m_s = 94(3)\ \text{MeV}. \tag{3}$$

Once these parameters are fixed, lattice QCD becomes a useful tool to calculate e.g. the low-energy constants for hadronic interactions [4]. One such interesting quantity is the strangeness content of the nucleon [5, 6]:

$$m_s\langle N|\bar{s}s|N\rangle < 60\ \text{MeV}, \quad y = \frac{2\langle N|\bar{s}s|N\rangle}{\langle N|\bar{u}u\bar{d}d|N\rangle} < 0.05. \tag{4}$$

These numbers are crucial for making a constraint on the spin-independent cross section between the nucleon and WIMP [7].

Lattice QCD can provide us with basic thermal properties of hot QCD matter, such as the order of the chiral transition, the (pseudo) critical temperature, and the equation of state. In the real world, the order of the chiral transition turns out to be the crossover from the finite scaling analysis of the chiral susceptibility [8]. In this case, the chiral condensate $\langle\bar{q}q\rangle_T$ changes smoothly as a function of temperature T, while its susceptibility has a peak around the pseudo critical temperature

$$T_{\rm pc} = 150 - 160\ \text{MeV}. \tag{5}$$

The previous discrepancy among different groups on the behavior of $\langle\bar{q}q\rangle_T$ comes from the lattice artifact originating from the finite lattice spacing (taste symmetry breaking) [9, 10].

The equation of state (pressure as a function of T) is a key quantity for relativistic hydrodynamics simulations to describe the space-time evolution of the hot QCD matter in relativistic heavy ion collisions. On the lattice, the pressure is obtained from the integration of the trace anomaly $\epsilon - 3P$ as

$$\frac{P(T)}{T^4} - \frac{P(T_0)}{T_0^4} = \int \frac{dT'}{T'}\frac{\epsilon(T') - 3P(T')}{T'^4}. \tag{6}$$

Depending on the method to improve the staggered fermion action, some discrepancy on the T dependence of $\epsilon - 3P$ can be seen in the present lattice QCD simulations, which should be resolved in the near future.

Since the suppression of the excited states of Υ (2S and 3S states) in heavy-ion collisions was found at the LHC [11], the fate of the heavy quarkoniums inside the quark-gluon plasma [12] has received renewed interests. The method of extracting the quarkonium spectral functions from lattice QCD using the maximal entropy method (MEM) formulated in [13] is a promising approach to attack this problem (see e.g. [14, 15]). To make definite conclusions, however, we need to carry out physical point simulations with larger temporal lattice data points.

3. Nuclear Lattice QCD

Understanding of the nuclear force from QCD is one of the most challenging problems in nuclear physics. Below the pion production threshold, the notion of the NN potential (either in coordinate space or in momentum space) is useful in the sense that it can be used not only to describe the two-body system but also to study nuclear many-body problems through ab-initio calculations [16]. Several high precision phenomenological NN forces have been constructed to reproduce the neutron-proton and proton-proton scattering data (about 4500 data points) with a $\chi^2/\mathrm{dof} \sim 1$. However, they have typically 20-40 fitting parameters: e.g. the CD Bonn potential, AV18 potential and N^{3}LO chiral effective field theory have 38, 40, and 24 parameters, respectively [17]. If one tries to extend these to hyperon-nucleon and hyperon-hyperon interactions, the task becomes extremely tough since the number of parameters increases and the scattering data are scarce.

In this situation, it is highly desirable to study the general baryon-baryon interactions from first principle lattice QCD simulations, since all the hadronic interactions in QCD are controlled only by the QCD scale parameter (Λ_{QCD}) and the quark masses (m_u, m_d, m_s) whose values are pretty well determined as mentioned before.

A theoretical framework to study the hadron-hadron interaction using lattice QCD was first proposed by Lüscher [18]: For two hadrons in a finite box with a size $L \times L \times L$ in the periodic boundary condition, an exact relation between the energy spectra in the box and the elastic scattering phase shift at these energies was derived. If the range of the hadronic interaction R is sufficiently smaller than the size of the box $R < L/2$, the behavior of the equal-time Nambu-Bethe-Salpeter (NBS) amplitude $\psi(\boldsymbol{r})$ in the interval $R < |\boldsymbol{r}| < L/2$ under the periodic boundary condition has sufficient information to relate the phase shift and the two-particle spectrum.

A different approach to the hadron interactions in lattice QCD was proposed by Ishii, Aoki and Hatsuda [19] and further developed by the HAL QCD Collaboration. Their starting point is the same equal-time NBS amplitude $\psi(\boldsymbol{r})$: Instead of looking at the amplitude outside the range of the interaction, the internal region $|\boldsymbol{r}| < R$ is considered and an energy-independent non-local potential $U(\boldsymbol{r}, \boldsymbol{r}')$ is defined from $\psi(\boldsymbol{r})$. Since $U(\boldsymbol{r}, \boldsymbol{r}')$ in QCD is a localized function in space due to the confinement of quarks and gluons, it is only weakly affected by the finite volume. Therefore, once U, although it is not a direct physical observable, is determined on the lattice, one may simply use the Schrödinger equation in the infinite space to calculate observables such as the scattering phase shifts, bound state spectra, resonance energies etc. In contrast to the direct application of the Lüscher's method (see e.g. [20]), the HAL QCD method enables us to make broader applications of lattice QCD results to nuclear physics. See the recent reviews, [21, 22] for details.

3.1. Lattice Nuclear Force

The NBS wave function for the nucleons in the HAL QCD method is defined as

$$\psi(\boldsymbol{r}, t) = \langle 0 | N(\boldsymbol{x} + \boldsymbol{r}, t) N(\boldsymbol{x}, t) | \mathcal{W} \rangle, \tag{7}$$

where $N(\boldsymbol{x}, t)$ is a local composite operator for the nucleon, with spin and isospin indices suppressed. $|\mathcal{W}\rangle$ is an exact QCD eigen state of 6 quarks with the total energy W. An important property of the NBS wave function $\psi(\boldsymbol{r}, t)$ is that its asymptotic behavior at large $|\boldsymbol{r}|$ in the infinite volume limit reproduces the correct phase shift obtained from the S-matrix of the elastic NN scattering. This can be shown explicitly by using the Nishijima-Zimmermann-Haag(NHZ)'s reduction formula [23] for the products of local composite operators.

One may choose any composite operators with the same quantum numbers as the nucleon to define the NBS wave function. Different interpolating operators lead to different NBS wave functions and different NN potentials. However, they lead to the same physical observables by construction. Analogous situation can be seen in quantum mechanics where the unitary

transformations modify both the wave function and the potential in such a way that observables are unchanged. An even more direct analogy is in field theory for point-like particles: Field re-definitions modify the vertices and propagators in the Feynmann rule, while the on-shell S-matrix is not affected by such changes.

The NN potential is defined as [19].

$$(E - H_0)\psi_{_E}(\boldsymbol{r}) = U_E(\boldsymbol{r})\psi_{_E}(\boldsymbol{r}) = \int U(\boldsymbol{r},\boldsymbol{r}')\psi_{_E}(\boldsymbol{r}')d\boldsymbol{r}'. \tag{8}$$

where $E = \boldsymbol{k}^2/m_N$ with $\boldsymbol{k}$ being the relative momentum defined from $W = 2\sqrt{\boldsymbol{k}^2 + m_N^2}$. The first equality is just a definition of the energy-dependent local potential, $U_E(\boldsymbol{r}) = K_E(\boldsymbol{r})/\psi_{_E}(\boldsymbol{r})$. On the other hand, the energy-independent non-local potential, $U(\boldsymbol{r},\boldsymbol{r}')$, is defined from $U_E(\boldsymbol{r})$ through a self-consistent equation,

$$U(\boldsymbol{r},\boldsymbol{r}') = \langle \boldsymbol{r}|\hat{U}|\boldsymbol{r}'\rangle = \sum_E \int_{-\infty}^{+\infty} \frac{dt}{2\pi} U_E(\boldsymbol{r})\langle \boldsymbol{r}|e^{i(\hat{H}_0+\hat{U}-E)t}|\boldsymbol{r}'\rangle. \tag{9}$$

Carrying out the t integration formally, one may also write Eq.(9) as $\hat{U} = \sum_E \hat{U}_E \delta(E - \hat{H}_0 - \hat{U})$.

In these formulae, $\sum_E$ stands for the summation (integration) over the discrete (continuum) energies. In particular, E is always discrete on the lattice with a finite volume. Also, E has an upper limit E_c at which inelastic scattering starts to take place. Eliminating the E-dependence of the potential through Eq.(9) has been discussed in a transparent manner by Królikowski and Rzewuski [24] a long time ago. Essentially the same method was rediscovered and discussed in [19] in the context of the NBS wave function on the lattice.

If we further focus on the low-energy scattering with E sufficiently smaller than the intrinsic scale of the system or the scale of the non-locality of the potential, the velocity expansion of $U(\boldsymbol{r},\boldsymbol{r}')$ in terms of its non-locality is useful [25]: For example, the potential with hermiticity, rotational invariance, parity symmetry, and time-reversal invariance may be expanded as [26]

$$U(\boldsymbol{r},\boldsymbol{r}') = V(\boldsymbol{r},\boldsymbol{v})\delta(\boldsymbol{r}-\boldsymbol{r}'), \tag{10}$$

$$V(\boldsymbol{r},\boldsymbol{v}) = \underbrace{V_C(r) + V_T(r)S_{12}}_{\rm LO} + \underbrace{V_{LS}(r)\boldsymbol{L}\cdot\boldsymbol{S}}_{\rm NLO} + \underbrace{O(\boldsymbol{v}^2)}_{\rm N^2LO} + \cdots, \tag{11}$$

where $\boldsymbol{v} = \boldsymbol{p}/\mu$ and $\boldsymbol{L} = \boldsymbol{r}\times\boldsymbol{p}$ with $\boldsymbol{p} = -i\nabla$, and $S_{12} = 3(\boldsymbol{\sigma}_1\cdot\boldsymbol{r})(\boldsymbol{\sigma}_2\cdot\boldsymbol{r})/r^2 - \boldsymbol{\sigma}_1\cdot\boldsymbol{\sigma}_2$.

Each coefficient of the expansion is a local potential and can be determined successively by measuring the NBS wave functions for several different energies. The central potential V_C and the tensor potential V_T are classified as the leading order (LO) potentials since they are of $O(\boldsymbol{v}^0)$. The next-to-leading (NLO) potential of $O(\boldsymbol{v})$ is the spin-orbit potential $V_{LS}(r)$.

To show that the above formulation works, (2+1)-flavour lattice QCD simulations have been performed for relatively heavy pion masses, $m_\pi = 411, 570, 701$ MeV [27]. It was found that the NN potential calculated on the lattice at low energy shows all the characteristic features expected from the empirical NN potentials obtained from the experimental NN phase shifts, namely the attractive well at long and medium distances and the repulsive core at short distance for the central potential. As for the tensor potential obtained from the coupled channel treatment of the $^3\mathrm{S}_1$-state and the $^3\mathrm{D}_1$-state, appreciable attraction at long and medium distances is found (see Fig.1).

As the quark mass decreases, the repulsive core and attractive well in the central potential, and the attractive well in the tensor potential tend to be enhanced. To make the deuteron bound, however, it is necessary to go the lighter quark masses toward the physical point. It was also shown that the derivative expansion in terms of the local and energy-independent potentials works well at low energies for at least the quark masses studies above [28].

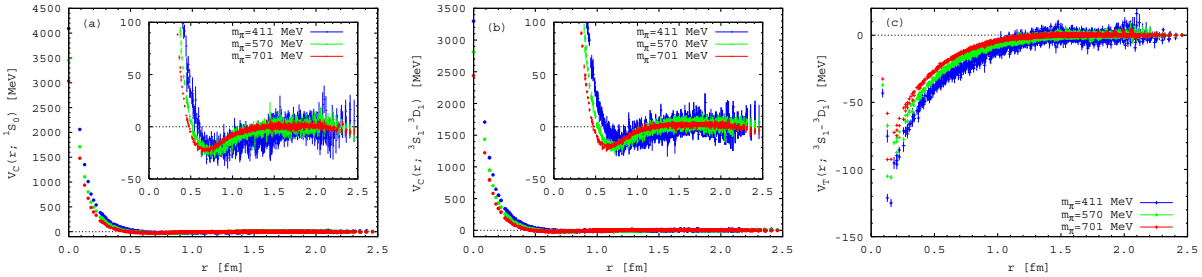

Figure 1. Quark mass dependence of the LO potentials in (2+1)-flavour QCD. (a) The central potential in the spin-singlet channel, (b) the central potential in the spin-triplet channel, and (c) the tensor potential in the spin-triplet channel [27].

There are a number of directions to be investigated on the basis of the HAL QCD approach. Among others, the most important direction is to carry out (2+1)-flavour simulations with a large volume ($L > 6$ fm) at the physical quark mass ($m_\pi = 135$ MeV) to extract the realistic NN potentials. This will be started soon at the 10 PFlops national supercomputer "KEI" which will have full operation in 2012 at the Advanced Institute for Computational Science (AICS) in Kobe, Japan [29]. Simulations of three or more nucleons on the lattice are also a challenging problem to be studied in relation to the attractive binding of finite nuclei and to the repulsive effect in high density matter relevant to neutron stars. Study along this line has been already started [30].

3.2. Lattice Baryon Forces

The origin of the repulsive core in the NN system can be clarified by considering the S-wave interaction between octet baryons in the flavour SU(3) limit. In this case, two baryon states with a given angular momentum are labelled by the irreducible flavour multiplets as

$$\mathbf{8} \otimes \mathbf{8} = \underbrace{\mathbf{27} \oplus \mathbf{8}_s \oplus \mathbf{1}}_{\text{symmetric}} \oplus \underbrace{\mathbf{10}^* \oplus \mathbf{10} \oplus \mathbf{8}_a}_{\text{anti-symmetric}} . \tag{12}$$

Here "symmetric" and "anti-symmetric" stand for the symmetry under the flavour exchange of two baryons.

For the system in the orbital S-wave, the Pauli principle between two baryons imposes **27**, $\mathbf{8}_s$ and **1** to be spin singlet ($^1S_0$) while $\mathbf{10}^*$, **10** and $\mathbf{8}_a$ to be spin triplet ($^3S_1$). Since there are no mixings among different multiplets in the SU(3) limit, one can define the corresponding potentials as

$$^1S_0 \quad : \quad V^{(\mathbf{27})}(r),\ V^{(\mathbf{8}_s)}(r),\ V^{(\mathbf{1})}(r), \tag{13}$$

$$^3S_1 \quad : \quad V^{(\mathbf{10}^*)}(r),\ V^{(\mathbf{10})}(r),\ V^{(\mathbf{8}_a)}(r) . \tag{14}$$

Potentials among octet baryons, both the diagonal part ($B_1B_2 \to B_1B_2$) and the off-diagonal part ($B_1B_2 \to B_3B_4$), are obtained by suitable combinations of $V^{(\alpha)}(r)$ with $\alpha = \mathbf{27}, \mathbf{8}_s, \mathbf{1}, \mathbf{10}^*, \mathbf{10}, \mathbf{8}_a$.

The NBS wave functions and the resultant potentials in this BB system show characteristic flavour dependence [31]: The potential $V^{(\mathbf{27})}$ which corresponds to the NN $^1S_0$ potential has a repulsive core at short distance and an attractive pocket as we have shown already in quenched and (2+1)-flavour simulations. On the other hand, $V^{(\mathbf{8}_s)}$ has a very strong repulsive core among all channels, and $V^{(\mathbf{1})}$ shows attraction for all distances (see the left panel of Fig.2.) These

features are consistent with what has been observed in phenomenological quark models [32]. In particular, the potential in the $\mathbf{8}_s$ channel in quark models becomes strongly repulsive at short distances since the six quarks cannot occupy the same orbital state due to quark Pauli blocking. On the other hand, the potential in the **1** channel does not suffer from the quark Pauli blocking and can become attractive due to short range gluon exchange.

Such an agreement between the lattice data and the phenomenological models indicates that the quark Pauli blocking plays an essential role for the repulsive core in BB systems as suggested long time ago in [33]. One can also confirm the idea of the Pauli blocking by considering the meson-baryon interaction such as the charmonium-nucleon potential [34] and the kaon-nucleon potential [35]. Generalization of the baryon-baryon interaction to the case with explicit SU(3) breaking is also under way [36].

3.3. H-dibaryon revisited

The H-dibaryon predicted by Jaffe [37] is a possible candidate for a bound dibayron with strangeness. Although a deeply bound H-dibaryon with a binding energy more than 7 MeV from the $\Lambda\Lambda$ threshold has been ruled out by the discovery of the double Λ hypernucleus, ^{6}He [38], there still remains a possibility of a shallow bound state or a resonance in the $(B, S, I) = (2, -2, 0)$ system. Although previous attempts have been made to calculate the binding energy of H-dibaryon from lattice QCD, they suffer from a serious finite volume effect: To accommodate two baryons inside the lattice volume, the spatial lattice size L should be large enough. Once L becomes large, however, energy levels of two baryons become dense, so that isolation of the ground state from the excited states becomes very difficult. This problem can be avoided by generalizing the original HAL QCD method to the (imaginary)time-dependent Schrödinger equation as shown in [39]. (For the direct application of the Lücher's method to the problem of H-dibaryon, see [41].)

From the 3-flavour QCD simulations with pion masss, $m_{NG} = 469, 672, 837, 1015, 1171$ MeV, it was found that H-dibaryon is a bound state with the binding energy ~ 20 MeV for the lightest pion mass $m_{NG} = 469$ MeV in the flavour SU(3) symmetric world [39]. The binding energy becomes smaller as the pion mass becomes smaller (see the right panel of Fig.2). This is due to the fact that the increase of the attraction toward the lighter quark mass is compensated by the increase of the kinetic energy for the lighter baryon mass. This gives us a boundary condition for the binding energy of H-dibaryon in the $m_K - m_\pi$ plane. To make a definite conclusion in the real world with explicit flavour SU(3) breaking, we need coupled channel analysis of the $\Lambda\Lambda - N\Xi - \Sigma\Sigma$ system in (2+1)-flavour lattice QCD simulations. Study along this direction is in progress [40].

4. Summary

Owing to the significant developments for past 10 years in both computational algorithms and the supercomputer performance, lattice QCD reached the level of (2+1)-flavour full QCD simulations with the pion mass $m_\pi = 135$ MeV, the lattice spacing $a \sim 0.05$ fm and the lattice volume $L \sim 6$ fm. Precise determination of the fundamental QCD parameters, the running coupling constant α_s and the quark masses m_q, became possible.

On the basis of this progress, quantitative calculations of the light hadron masses, low energy QCD constants, pseudo-critical temperature and the equation of state of hot QCD come within reach. Lattice QCD is also useful to determine key parameters (such as the strangeness content of the nucleon) needed to make constraints on the theories beyond the standard model.

Lattice QCD also provides some qualitative understanding of the many-body problem of quarks and gluons. The origin of the nuclear force and hyperon forces from full QCD simulations are among the top highlights of the recent progress in this direction. The low-energy baryon-baryon potentials obtained from the Nambu-Bethe-Salpeter amplitude on the lattice (HAL QCD

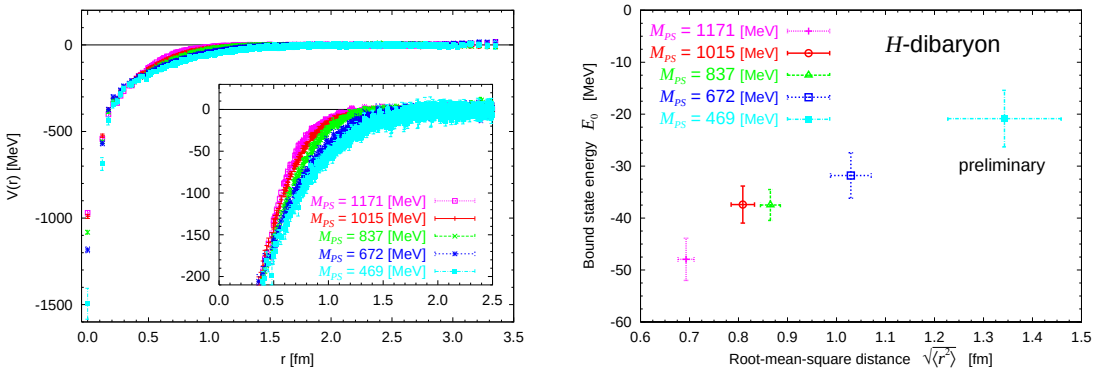

Figure 2. Left: Potential in the flavour-singlet BB channel. Right: Binding energy and the size of the H-dibaryon. Taken from [39].

method) play key roles in the construction of a firm QCD basis of nuclear physics. Furthermore, this method can be applied to the potential between heavy quarks, which could make a firm QCD basis of the phenomenological quark models for charmoniums and bottomoniums [42, 43].

In a few years, we would (like to) see physical point simulations for many observables by using Pflops class supercomputers. Among others, the determination of the two-baryon and three-baryon forces at the physical point is most important and urgent from the point of view of nuclear physics and neutron star structure. Simulations with fermions having better chiral symmetry such as the domain wall fermion and overlap fermion will eventually replace the current simulations with improved staggered fermions and improved Wilson fermions.

After 100 years of the discovery of atomic nuclei by Rutherford, it is probably not too much of an exaggeration to say that we are about to understand the structure of atomic nuclei and neutron stars from the fundamental law of the strong interaction, the quantum chromodynamics.

Acknowledgments

TH was supported in part by the Grant-in-Aid for Scientific Research on Innovative Areas (No 2004: 20105003) and the by Japanese MEXT grant (No 22340052).

References

[1] Aoki S *et al.* [PACS-CS Collaboration] 2010 *Phys. Rev.* **D81** 074503
[2] Durr S *et al.* [BMW Collaboration] 2011 *JHEP* **1108** 148
[3] Shintani E Talk at Lattice 2011.
[4] Juttner A *et al.* [FLAG Collaboration] 2011 arXiv:1109.1388 [hep-ph]
[5] Giedt J, Thomas A W, Young R D 2009 *Phys. Rev. Lett.* **103** 201802
[6] Takeda K *et al.* [JLQCD Collaboration] 2011 *Phys. Rev.* **D83** 114506
[7] Aprile E *et al.* [XENON100 Collaboration] 2011 arXiv:1107.2155 [astro-ph.IM]
[8] Aoki Y, Endrodi G, Fodor Z, Katz S D, Szabo K K 2006 *Nature* **443** 675
[9] Borsanyi S *et al.* [Wuppertal-Budapest Collaboration] 2011 arXiv:1109.5032 [hep-lat]
[10] Bazavov A *et al.* [HotQCD Collaboration] 2011 arXiv:1107.5027 [hep-lat]
[11] Chatrchyan S *et al.* [CMS Collaboration] 2011 *Phys. Rev. Lett.* **107** 052302
[12] Matsui T, Satz H 1986 *Phys. Lett.* **B178** 416
[13] Asakawa M, Hatsuda T, Nakahara Y 2001 *Prog. Part. Nucl. Phys.* **46** 459
[14] Ding H T, Francis A, Kaczmarek O, Karsch F, Satz H, Soeldner W 2011 arXiv:1107.0311 [nucl-th]
[15] Aarts G, Allton C, Kim S, Lombardo M P, Oktay M B, Ryan S M, Sinclair D K, Skullerud J I 2011 arXiv:1109.4496 [hep-lat]
[16] Epellbaum E *et al.* 2009 *Rev.Mod.Phys.* **81** 1773
Brown G E, Kuo T T S, Holt J W, Lee S 2010 *The Nucleon-Nucleon Interaction and the Nuclear Many-Body Problem* (World Scientific, Singapore).

[17] Machleidt R 2007 arXiv:0704.0807 [nucl-th]
[18] Lüscher M 1991 *Nucl. Phys.* B **354** 531
[19] Ishii N, Aoki S, Hatsuda T 2007 *Phys. Rev. Lett.* **99** 022001
Aoki S, Hatsuda T, Ishii N 2010 *Prog. Theor. Phys.* **123** 89
[20] Beane S R *et al.* [NPLQCD Collaboration] 2010 *Phys. Rev.* **D81** 054505
[21] Aoki S *Lecture at Les Houches Summer School on "Modern perspectives in lattice QCD"* 2010 arXiv:1008.4427 [hep-lat]
[22] Hatsuda T 2010 *PoS* **LAT2010** 008
[23] Nishijima K 1958 *Phys. Rev.* **111** 995
Zimmermann W 1958 *Nuovo Cim.* **10** 597
Haag R 1958 *Phys. Rev.* **112** 669
See also, Zimmermann W 1987 MPI-PAE/PTh-61/87 (unpublished)
[24] Królikowski W, Rzewuski J 1956 *Nuovo Cimento* **4** 1212
[25] Tamagaki R, Watari W 1967 *Prog. Theor. Phys. Suppl.* **39** 23
[26] Okubo S, Marshak R E 1958 *Ann. of Phys.* **4** 166
[27] Ishii N [PACS-CS and HAL QCD Collaborations] 2009 *PoS* **LAT2009** 019
[28] Murano K, Ishii N, Aoki S, Hatsuda T 2011 *Prog. Theor. Phys.* **125** 1225
[29] `http://www.aics.riken.jp/index.html`
[30] Doi T *et al.* [HAL QCD Collaboration] 2011 arXiv:1106.2276 [hep-lat]
[31] Inoue T *et al.* (HAL QCD collaboration) 2010 *Prog. Theor. Phys.* **124** 591
[32] See e.g. Oka M, Shimizu K, Yazaki K 2000 *Prog. Theor. Phys. Suppl.* **137** 1
Fujiwara Y, Suzuki Y, Nakamoto C 2007 *Prog. Part. Nucl. Phys.* **58** 439
[33] Otsuki S, Yasuno M, Tamagaki R 1965 *Prog. Theor. Phys. Suppl.* Extra Number **1965** 578
Machida S, Namiki M 1965 *Prog. Theor. Phys.* **33** 125
[34] Kawanai T, Sasaki S 2010 *Phys. Rev.* D **82** 091501
[35] Ikeda Y (for HAL QCD Collaboration) 2010 *Prog.Theor.Phys.Suppl.* **186** 228
[36] Nemura H (for HAL QCD and PACS-CS Collaborations) 2011 *Few Body Syst.* **50** 105
[37] Jaffe R L 1977 *Phys. Rev. Lett.* **38** 195; *Erratum-ibid.* **38** 617
[38] Takahashi H *et al.* 2001 *Phys. Rev. Lett.* **87** 212502
[39] Inoue T *et al.* [HAL QCD Collaboration] 2011 *Phys. Rev. Lett.* **106** 162002
Inoue T (for HAL QCD Collaboration) 2011 arXiv:1109.1620 [hep-lat]
[40] Sasaki K (for HAL QCD Collaboration) 2010 *PoS* **LAT2010** 157
[41] Beane S R *et al.* [NPLQCD Collaboration] 2011 *Phys. Rev. Lett.* **106** 162001
[42] Ikeda Y, Iida H 2011 arXiv:1102.2097 [hep-lat]
[43] Kawanai T, Sasaki S 2011 *Phys. Rev. Lett.* **107** 091601; arXiv:1110.0888 [hep-lat]